IRAQI BULLETIN OF GEOLOGY AND MINING (IBGM)\
IRAQ GEOLOGICAL SURVEY (GEOSURV-IRAQ)

*IBGM (**2025**, Vol; Issue)* *455-477*

KINEMATIC AND GEOLOGICAL STRENGTH INDEX-SLOPE APPLICATION FOR STABILITY EVALUATION OF THE ROCK SLOPES FOR SOME SELECTED SITES ALONG OLD AZMAR ROAD IN A PART OF AZMAR ANTICLINORIUM, SULAIMANIYAH, KURDISTAN REGION NE-IRAQ

Ghafor A. Hamasur*, Salim H. Sulaiman, and Fahmy O. Mohammed

Department of Geology, College of Science, University of Sulaimani,
***** *Corresponding author e-mail:* ghafor.hamasur@univsul.edu.iq

Type of the Paper (Article)
Received: 02/ 08/ 2024
Accepted: 14/ 04/ 2025
Available online: 27/ 06/ 2025

Abstract

This study comprises choosing ten (10) excavated rock slope stations along old Azmar road, on the NE-side of Azmar mountain at Sulaymaniyah, Kurdistan region, NE-Iraq, and the stability of these excavated rock slopes was evaluated by descriptive and quantitative approaches. The selection of the slope stations relies on changes in the discontinuity type, slope steepness and orientation, and failure type. The field data was analyzed to determine its possible type of instability, employing the slope kinematics method by the DIPS v6.008 program, and to verify the stability condition, the Geological Strength Index-slope (GSI_{slope}) system Finally, the joints were geometrically classified, based on the three (3) orthogonal geometric axes. Geometrical classification of joints revealed an ac-joint set, and hko>a, hko>b, hol>c & okl>c joint system. The most prevalent type is of conjugate hko joint system, whereas there are no conjugate joint systems of hol>a & okl>b types. Kinematic analysis showed four failure types, i.e., planar sliding, wedge sliding, flexural, and direct toppling failures. Planar slides may occur on the rock slopes of stations no. 2, 3, 4, 5, 6, 7, 8, 9, and 10, wedge sliding may occur on the rock slopes of stations no. 1, 8, and 9, flexural and direct toppling may occur on the rock slope. The results of the GSI-slope showed that the rock slopes in stations 3 and 5 are in the completely unstable condition of class no. Five (V), and stations no. 1, 2, 4, 6, 7, 8, and 9 are in the unstable condition of class four (lV), while the slope in station no. 10 is in a partially stable condition of class three (III).

Keywords: Joint geometry; Road hazard; Rock Slope stability; RMR; Western Zagros; Kurdistan; Iraq.

ISSN 1811-4539, EISSN 3005-3714
https://doi.org/10.59150/ibgm2101a24
IBGM: http://ibgm-iq.org/
Academic Scientific Journals: www.iasj.net

1. Introduction

Roads and highways in the Iraqi Kurdistan mountainous areas are important in the remote transport system. Any instability in the slopes may lead the traffic to get worse and bring seriousness to people. Also, the study of rock slope stability aids the successful excavation designing of rock slopes for road construction or expansion purposes and maintaining other engineering projects in a safe state.

Quite many researchers such as (Chakraborty & Dey, 2019; Hamasur, 2022; Hoek & Bray, 1981; Hostani & Hamasur, 2022; Marinos et al., 2005; Pantelidis, 2009; Sharma et al., 2019); studied the stability of slopes along road-cut slopes that join remote areas with towns and cities. Also, other engineering geological studies used the landslide possibility index (LPI) method (Al-Saadi, 1981; Hamasur, 2013; Janardhana et al., 2018; Mohammed et al., 2020).

The slope failures in mountainous areas are the most abundant geological hazard. There are main factors that lead to slope failures among them are anthropogenic activities such as cutting steep slopes, blasting, road widening, and trimming trees around the roads (Al-Bared et al., 2019; Hussien et al., 2020; Huang et al., 2022; Malviya et al., 2024). The natural condition of slopes and discontinuities also affect the slope stability of the detached masses (Mohammed et al., 2023). The rock mass classification systems and methods are also essential tools in the evaluation of slope failure, especially the kinematic method, slope mass ratings (SMR), Q-slope, and Geological Strength Index-slope (GSI-slope) (Hoek & Bray, 1981; Romana, 1985; Bar & Barton, 2017; Hamasur, 2023; Hamasur & Qadir, 2020;). The assessment of road stability in the mountainous area, especially in the northeastern part of Iraq is very crucial because the road network is the backbone of the economy and tourism for the Iraqi government and its people (Hamasur et al., 2020). The road network in the Azmar area is a single carriageway that contains many unstable slopes which are made by man-made excavated slopes during road widening, also due to the tectonic condition (intense folding and discontinuities steep dip angle) of the Azmar anticline which is located at the unstable margin of the Arabian plate (Aziz et al., 2001; Buday, 1980; Fouad, 2015; Jassim & Goff, 2006 Al-Hakary, 2011).

The area under study is about 17-20 km to the northeast of Sulaimaniyah, city/NE-Iraq, and between latitudes 35°38′45″ N – 35°28′55″ N and longitudes 45°38′08″ E – 45°38′40″ E, as in Figure (1).

This study aims to use the kinematic method and GSI_{slope} system to determine the probability of failure types and the degree of stability conditions of ten (10) excavated rock slopes along the old Azmar road.

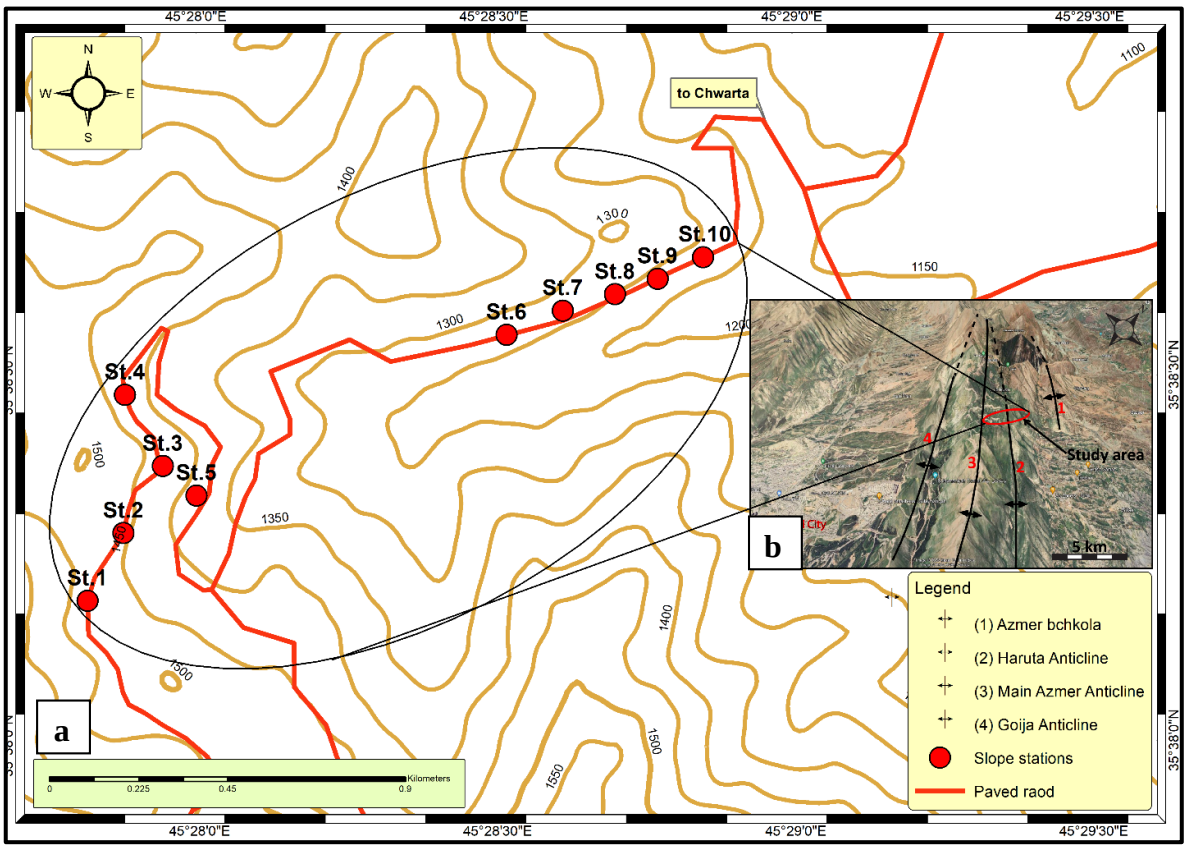

Figure 1. a) The studied traverse location map, b) Google map of Azmer anticlinorium b.

2. Geological Setting of the study area

2.1. Stratigraphy

All the exposed rocks in the Azmar anticlinorium are of the Cretaceous period. The oldest is the Balamabo Formation exposed at the core of the Azmar anticlinorium, which is composed of marly limestone and grey marl, overlain by the Kometan Formation, which is composed of white well-bedded fine-grain limestone (Karim and Ahmad, 2014). These last two formations reflect a high magnitude of deformations and form the carapace of the fold. On both limbs, the Kometan Formation is overlain by the Shiranish Formation, which consists of an alternation of light and bluish-white marl and marl limestone (Buday, 1980).

2.2. Tectonics and Structure

The study area is located in a part of the Azmar anticline anticlinorium which belongs to the imbricated zone (Aziz et al., 2001; Buday, 1980; Jassim & Goff, 2006; Omar et al., 2015; Stevanovitic et al., 2003) This structure seems to be an anticlinorium because it is composed of more than one-fold, and is considered to be one of the huge structures within the imbricate zone of the Zagros Fold Thrust Belt (Numan, 1997, Aziz et al., 2001; Jassim & Goff, 2006;). Azmar anticlinorium is located nearly 17 – 20 km northeast-east of Sulaimaniyah city. The highest point on the main Azmir fold exceeds 1700 m above sea level. The fold trend is NW – SE within the Zagros fold trend; the fold reflects high complexity in structure. It is

asymmetrical; the southwestern limb of the main Azmir fold is overturned toward the northeast for about 20 degrees. The structure's length approaches 50 km and the width is about 4 km. Azmar anticlinorium consists of a series of anticlines and synclines that are from northeast towards southwest as follows, Azmar Bechkola anticline, at the most upper northeastern side, the Haruta anticline, and the main Azmar anticline at the middle part, while Goizha anticline located at the lowermost southwest side (Al-Hakary, 2011; Aziz et al., 2001; Lawa et al., 2013; Stevanovitic et al., 2003) as in Figure 2.

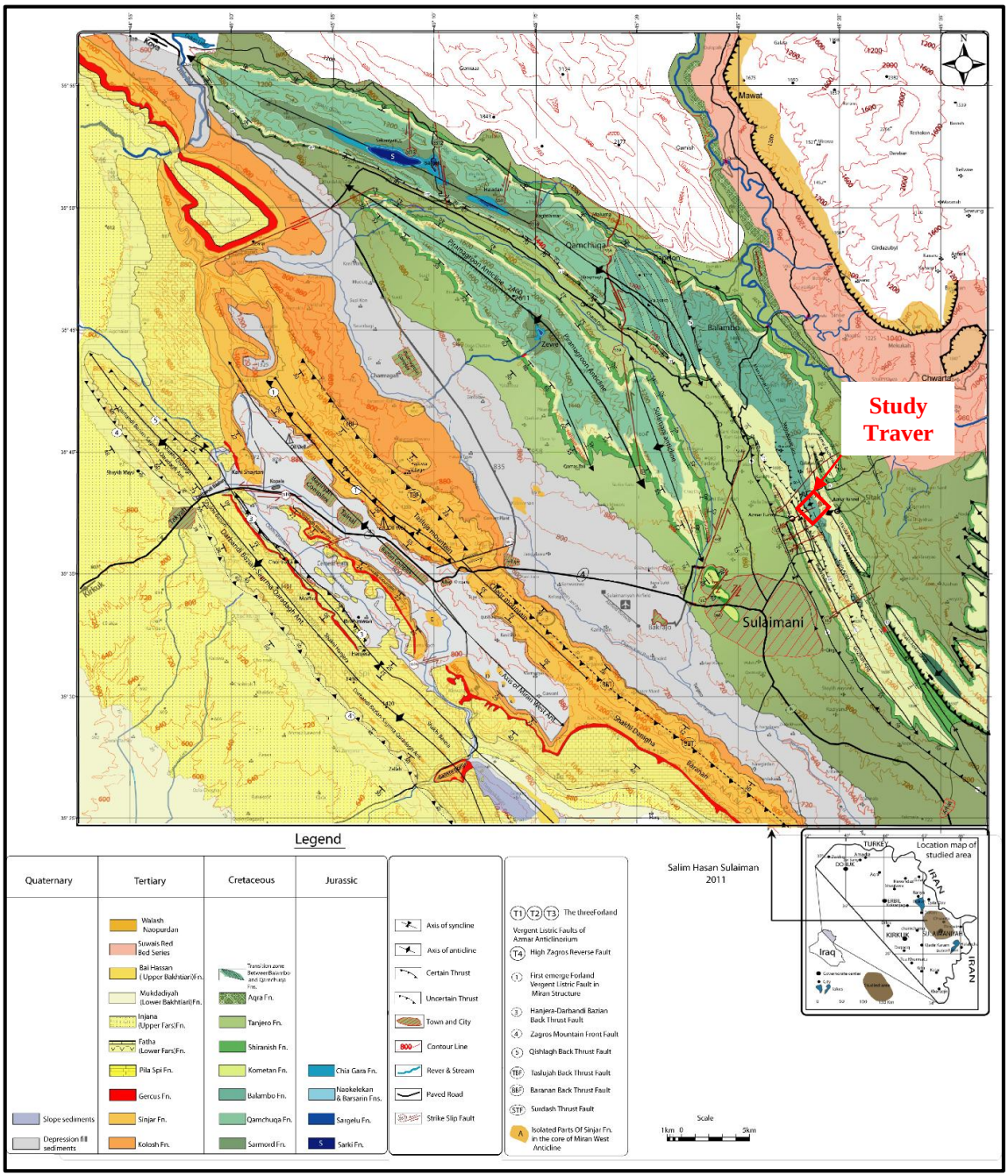

Figure 2. Geological map of Azmar-Goizha Piramagron, Surdash anticlines, after (Al-Hakary, 2011), the same map was also published by Omar et al. (2015).

2.3. Geometric analysis of fractures in the study area

Geometric analysis of fractures (joints) in rocks involves studying the characteristics and patterns of fractures within rock formations. This analysis is important in various fields, including geology, engineering geology, and geotechnical engineering (Turner & Weiss 1963).

The fieldwork was carried out through 10 stations along the old Azmar road as shown in Table 2. The collected data included the attitude of bedding planes, joints, and slopes with a friction angle of the possible failure surface, as in Table 2.

Table 1. Geographic coordinates, geologic Formation, and position of the ten (10) rock slope stations.

Station no.	Latitude	Longitude	Elevation (a.s.l) m	Formation	Position
1	35° 38' 14.6"	45° 27' 50.2"	1453	Balambo	SW – limb of Azmer Anticlinorium
2	35° 38' 20.7"	45° 27' 53.8"	1433	Balambo	
3	35° 38' 22.9"	45° 27' 56.4"	1426	Balambo	
4	35° 38' 25.9"	45° 27' 54.9"	1416	Balambo	
5	35° 38' 19.7"	45° 28' 01.1"	1356	Balambo	NE – limb of Azmer Anticlinorium
6	35° 38' 33.3"	45° 28' 32.6"	1260	Balambo	
7	35° 38' 34.4"	45° 28' 36.4"	1256	Kometan	
8	35° 38' 37.1"	45° 28' 44"	1250	Kometan	
9	35° 38' 37.5"	45° 28' 44.8"	1235	Kometan	
10	35° 38' 38.9"	45° 28' 48.1"	1227	Kometan	

Joints on the bedding plane were classified depending on the geometrical relation with the three perpendicular geometric axes (a, b & c). Software (DIPS V6.008) was used for constructing the data of bedding planes as great circles and joint planes as poles to find the geometric relationships and classify the joints into extension sets and shear systems, according to Hancock and Atiya, (1979), this classification is used by Turner & Weiss (1963) and followed by Al-Jumaily, (2004), Bieniawski (1973), Bieniawski (1989), Hancock (1985), Hancock et al. (1984), Markland (1972), and Ramsay & Huber (1987).

The excavated slopes are characterized by steep to very steep inclinations with an obvious discontinuity system, as in Table 2. The geometrical classification of joints in the ten stations, revealed an ac-joint set, and hko>a, hko>b, hol>c & okl>c joint system. The most prevalent type is of conjugate hko joint system, whereas there are no conjugate joint systems of hol>a & okl>b types, as in Figure 3.

Table 2. Attitude of slope, discontinuities, and friction angle in the ten (10) slope stations.

Slope station no.	Formation	Slope direction/ slope angle	Bedding dip direction/ Dip angle	Joint set (J1) Dip direction/ Dip angle	Joint set (J2) Dip direction/ Dip angle	Joint set (J3) Dip direction/ Dip angle	Friction angle (ϕ)
1 (La)	Balambo	115°/60°	065°/55°	140°/80°	242°/26°		32°
1 (Lb)			200°/65°	125°/75°	055°/28°		
2		105°/60°	242°/50°	087°/58°	165°/82°		32°
3		076°/53°	070°/50°	150°/84°	205°/54°	270°/45°	32°
4		048°/68°	048°/68°	227°/45°	140°/85°	310°/60°	32°
5	Balambo	125°/60°	040°/80°	140°/36°	120°/80°	311°/66°	32°
6		160°/80°	250°/82°	160°/80°	035°/30°		34°
7		172°/80°	080°/80°	172°/80°	263°/50°		34°
8	Kometan	175°/76°	275°/46°	115°/46°	170°/74°		33°
9		135°/62°	275°/48°	120°/56°	200°/80°		34°
10		175°/72°	060°/38°	170°/72°	237°/35°		34°

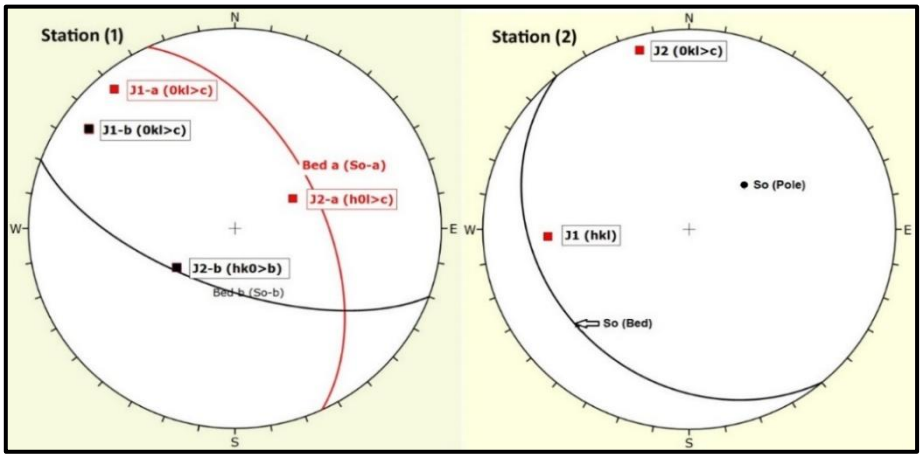

Figure 3. Geometric classification of joints in the rock slope stations 1 and 2.

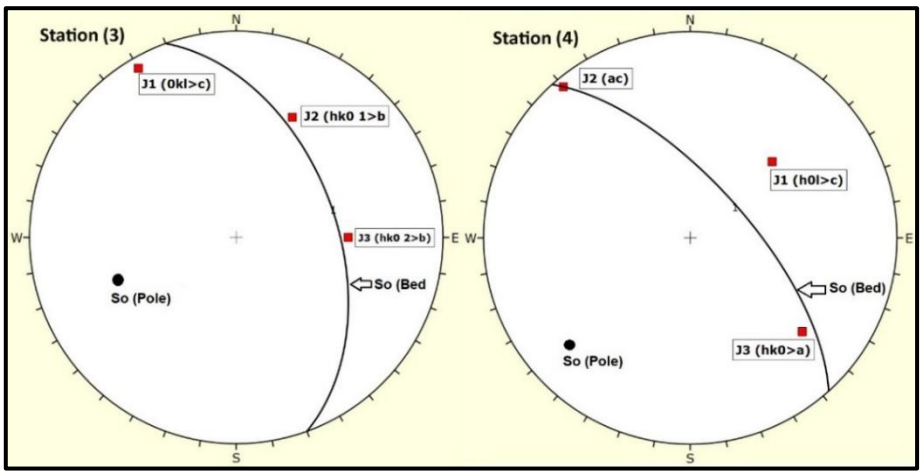

Figure 3 Continuer. Geometric classification of joints in the rock slope stations 3 and 4.

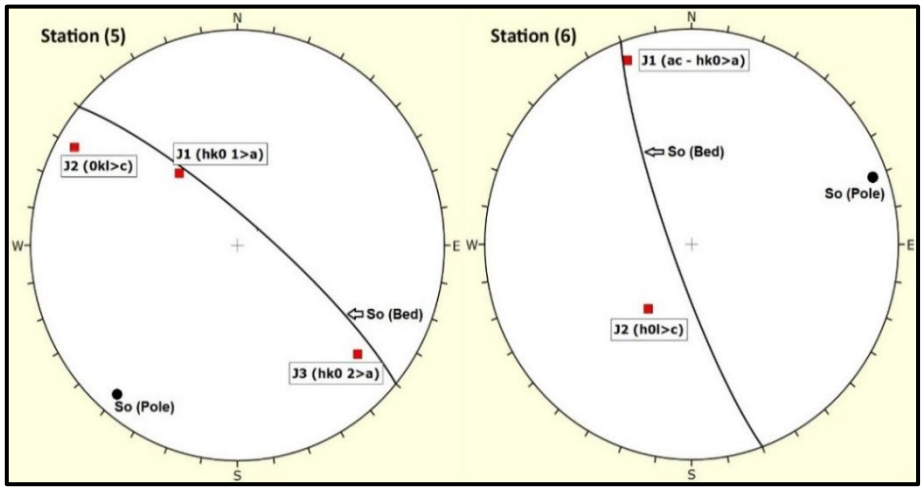

Figure 3 Continuer. Geometric classification of joints in the rock slope stations 5 and 6.

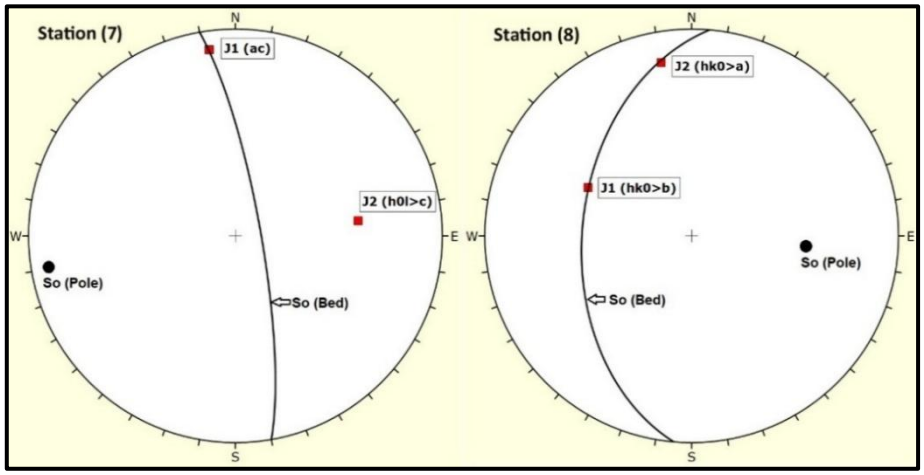

Figure 3 Continuer. Geometric classification of joints in the rock slope stations 7 and 8.

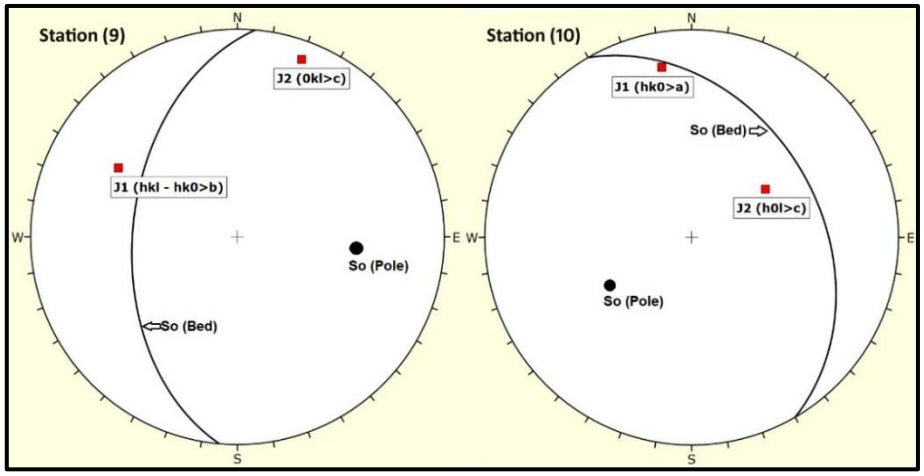

Figure 3 Continuer. Geometric classification of joints in the rock slope stations 9 and 10.

3. Materials and Methods

Detail engineering geological and structural analysis was done for ten (10) excavated rock slopes. The survey included detailed joint analysis, slope measurement, and bedding attitudes. The field observation was used for the kinematic analysis and GSI_{slope} system for all studied slopes.

The kinematic method is a simple practice way for identifying probable types of failure (plane, wedge, and toppling) from the angular relationship between discontinuities and the slope face, using stereographic analysis (Al-Saadi, 1981; Hoek & Bray, 1981; Pantelidis, 2009).

The wedge mass may slide along the intersection line of two planes, and it can cause a wedge sliding, (Markland, 1972; Singh & Goel, 1999) is one of the kinematic techniques for evaluating this type of failure. (Hocking, 1976) modified and explained the Markland method to differentiate between wedge sliding and plane sliding. When a steeply dipping discontinuity is parallel or subparallel to the slope surface (within ±30°) and dips inwards it is characteristic of flexural toppling (Goodman, 1989), block toppling needs the converging of two geologic planes to establish detached masses, also, the basal surface presence promotes the occurrence of block toppling.

The field measurements of the discontinuities and slope were analyzed by DIPS v6.008 software of *Rocscience Inc. Dip v. 6.008* (2015) to graphically determine the possible failure types. The cohesion of a planar and clean (no infilling) discontinuity is considered to be zero, and the shear strength of a possible failure surface is specified primarily by the friction angle. The sliding friction angles of discontinuities were estimated in the field, using the (Bruce et al., 1989), tilting method, as in Figure 4, and they are between 32° – 34°.

The Kinematic analysis GSI_{slope} systems were used by several researchers, such as Al Jubory et al. (2022), Hamasur (2023), Hasan & Abood, 2024, and Qader & Syan (2021) and are a very applicable tool for direct stability evaluation of rock slopes in the field, it's also uses a Geological Strength Index (GSI) chart of Marinos & Hoek (2000) for determining the GSI values of rock masses in the field, as input for determining the value of GSI_{slope} as in equation1:

$$GSI_{slope} = GSI\text{-}10 + GW + (F1 \times F2 \times F3) \quad (1)$$

Where: GSI is the geological strength of rocks, and F1 is the rating of the declination of the discontinuity orientation (or plunge orientation of two geological planes) from slope orientation. F2 is the rating of the discontinuity dip angle or plunge inclination of the intersection line of two discontinuities. F3 is the rating of the difference between the discontinuity dip angle and slope inclination (for planar sliding) or between the plunge inclination of two discontinuities intersection line and slope inclination (for wedge sliding), and F3 in the case of toppling is the rating of the sum for both discontinuity angle and slope inclination (for flexural toppling) or the sum of the plunge angle and slope inclination (for direct

toppling) (Hamasur et al., 2020; V. Marinos et al., 2005; V. Marinos & Carter, 2018). F1, F2 & F3 are easily calculated using charts which are used by Hamasur (2023), as in Figure 5.

GSI_{slope} can be measured from Eq.1 by subtracting the value of 10 (ten) and the product of the three-factor multiplication (F1, F2 & F3) from GSI and adding field groundwater rating parameter (GW) from Bienawski (1976)Table. Finally, the stability condition and its class can be determined from the GSI_{slope} value, as in Table 3, based on the Romana (1985) slope mass rating system has been adapted to use GSI_{slope} values instead.

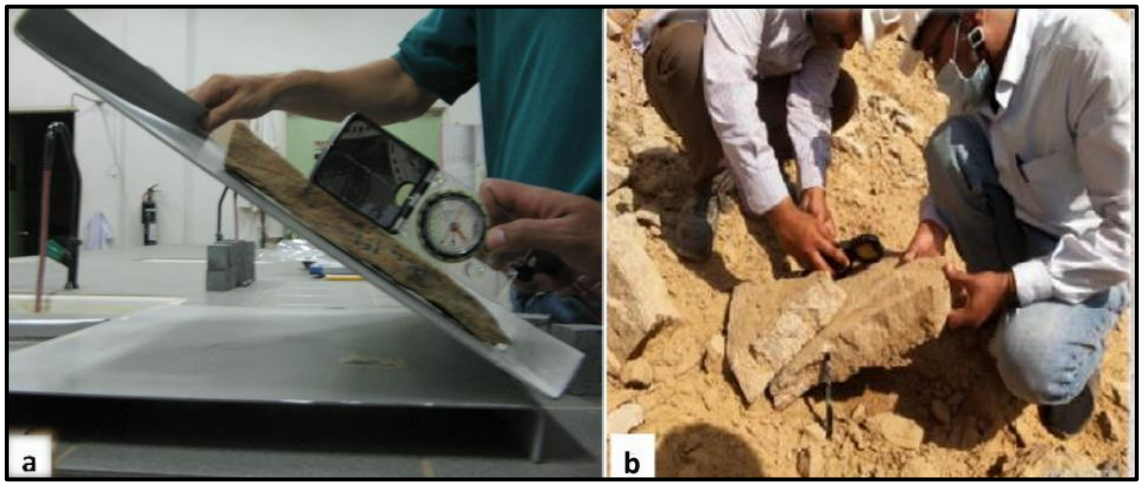

Figure 4. a) A tilt testing device, (Modified from Bruce, et al. (1989) by Priest (1993); b) Measuring friction angle of discontinuity in the field (Meena et al., 2025).

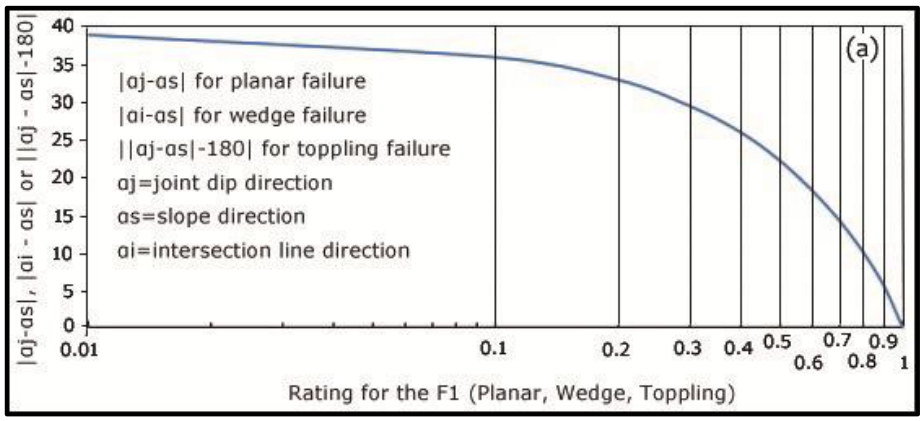

Figure 5a. Chart for determining the rating of the F1 adjustment factor for planar, wedge, and toppling failures (Hamasur, 2023).

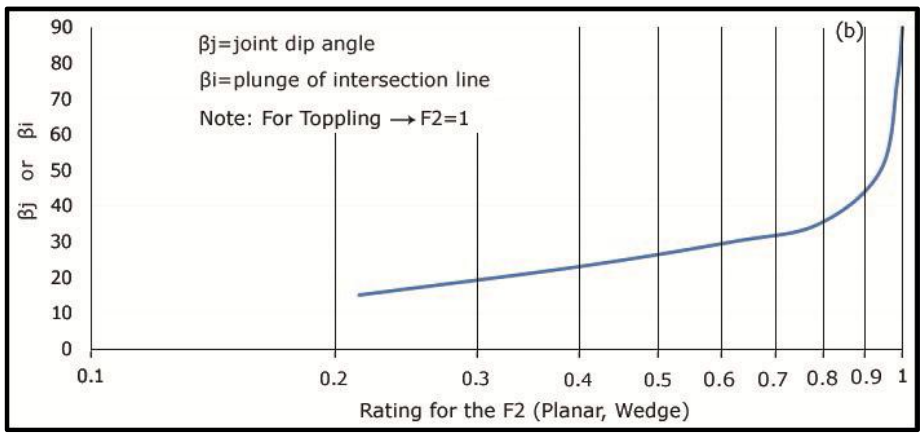

Figure 5b. Chart for determining the rating of the F2 adjustment factor for planar and wedge failures (Hamasur, 2023).

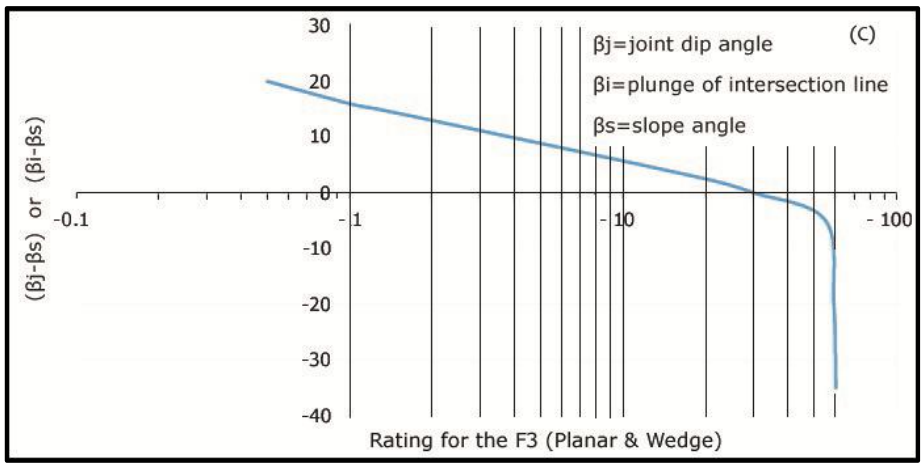

Figure 5c. Chart for determining the rating of the F3 adjustment factor for planar and wedge failures (Hamasur, 2023).

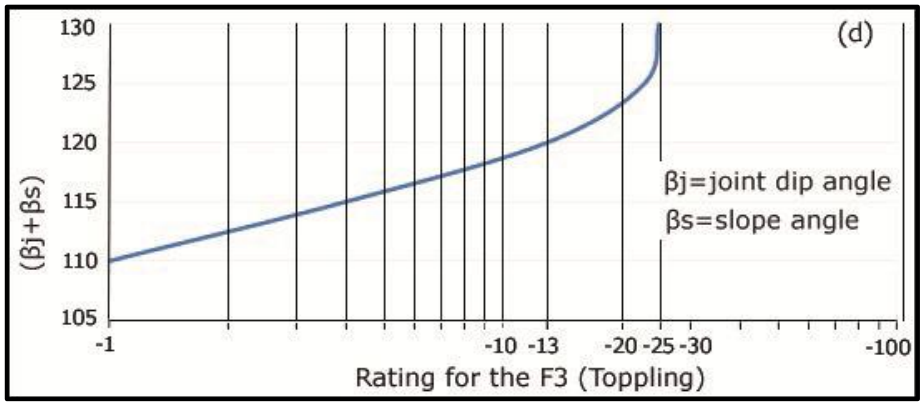

Figure 5d. Chart for determining the rating of the F3 adjustment factor for toppling failure (Hamasur, 2023).

Table 3. Description of GSI*slope* stability classes and conditions [Modified from Romana (1985) after Hamasur, 2023].

GSI_{slope} value	**100←81**	**80←61**	**60←41**	**40←21**	**< 21**
Stability class	I	II	III	IV	V
Stability condition	Completely stable	Stable	Partially stable	Unstable	Completely unstable

4. Results and Discussion

The excavated rock slopes are good sites for determining the changes in lithology, weathering states, and outcrops characteristics of the geological structures to record various discontinuities (bedding, joints, faults, ….. etc). This study consists of an investigation of ten (10) excavated rock slopes that have different structural and geomorphological properties.

The excavated slopes consisted of a succession of marly-limestone and marl (stations no. 1, 2, 3, 4 & 5, or thin-intermediate beds of limestone (stations no. 6, 7, 8, 9 & 10). Very steep to steep inclination is the characteristic of the excavated slopes with existing discontinuity sets and systems, as in Table 2.

Kinematic analysis of the excavated slopes was carried out using DIPS v6.008 (Rocscience, 2015). The potential failure zones are indicated in purple across all ten stations in the analysis. The orientation of discontinuities relative to the slope suggests the presence of planar, wedge, and toppling failure modes. According to the kinematic analysis results, planar sliding is likely to occur at stations 2 through 10, as illustrated in Figures (7b, 8b, 9b, 10b, 11b, 12b, 13b, and 14b). Wedge sliding is predicted at stations 1, 8, and 9, as seen in Figures (6b, 13c, and 14c). Additionally, station 5 exhibits potential for both flexural and direct toppling failures, represented in Figures 10c and 10d, respectively.

All excavated rock slopes are locations that previously failed, as in Figures (6a, 7a, 8a, 9a, 10a, 11a, 12a, 13a, 14a, and 15a). The stereographic analysis results of all stations are arranged in Table 4.

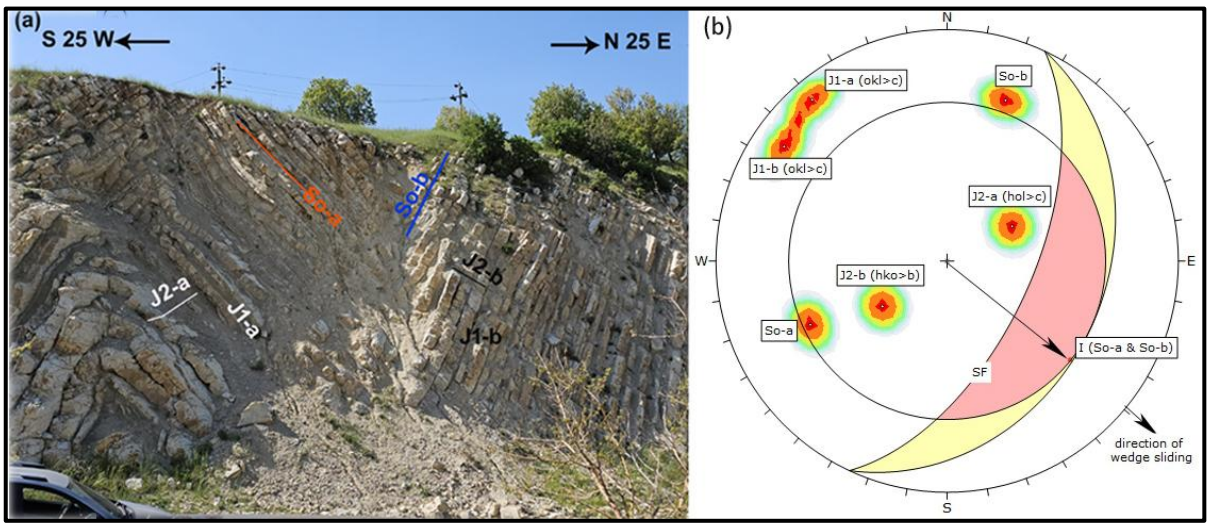

Figure 6. a) Photo of Station No. 1 with signs for discontinuity groups. B) Stereographic analysis displays wedge sliding on So-a and So-b (a and b are the two limbs of the minor syncline). Where: SF = slope face; So = bedding plane; J1 = joint set no.1; J2 = joint set no.2, the purple color is a probable failure area.

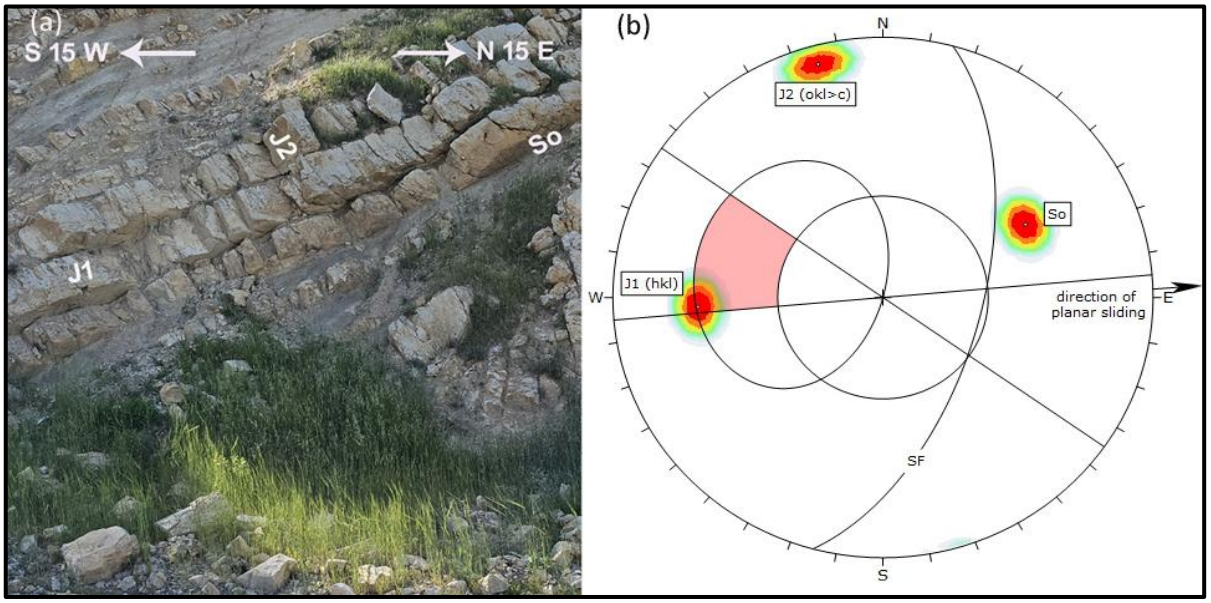

Figure 7. a) Photo of Station No.2 with signs for discontinuity groups. b) Stereographic analysis displays planar sliding on J1.

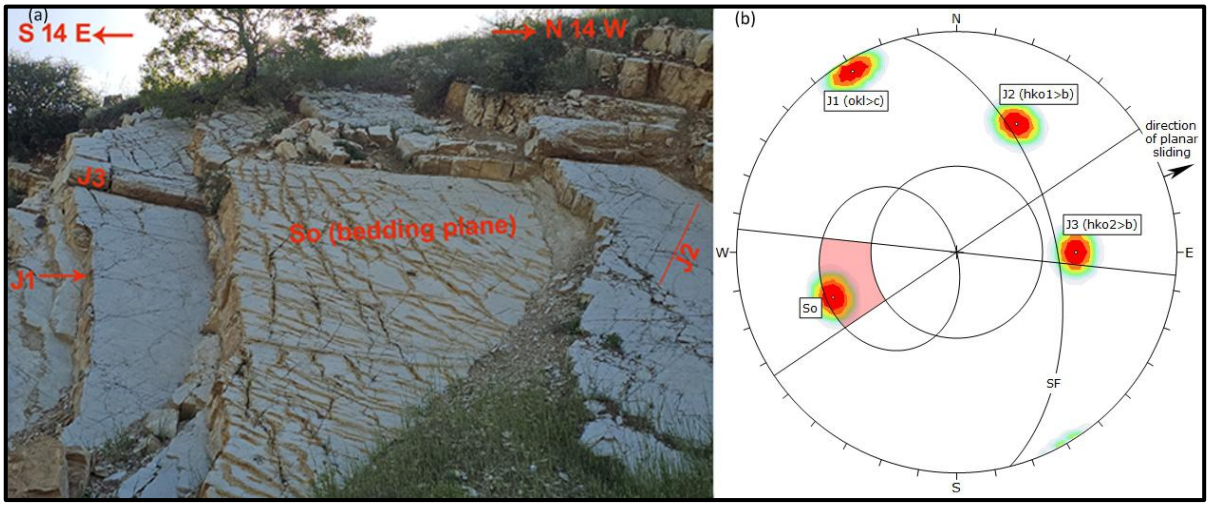

Figure 8. a) Photo of Station No. 3 with signs for discontinuity groups. b) Stereographic analysis displays planar sliding on So (bedding plane).

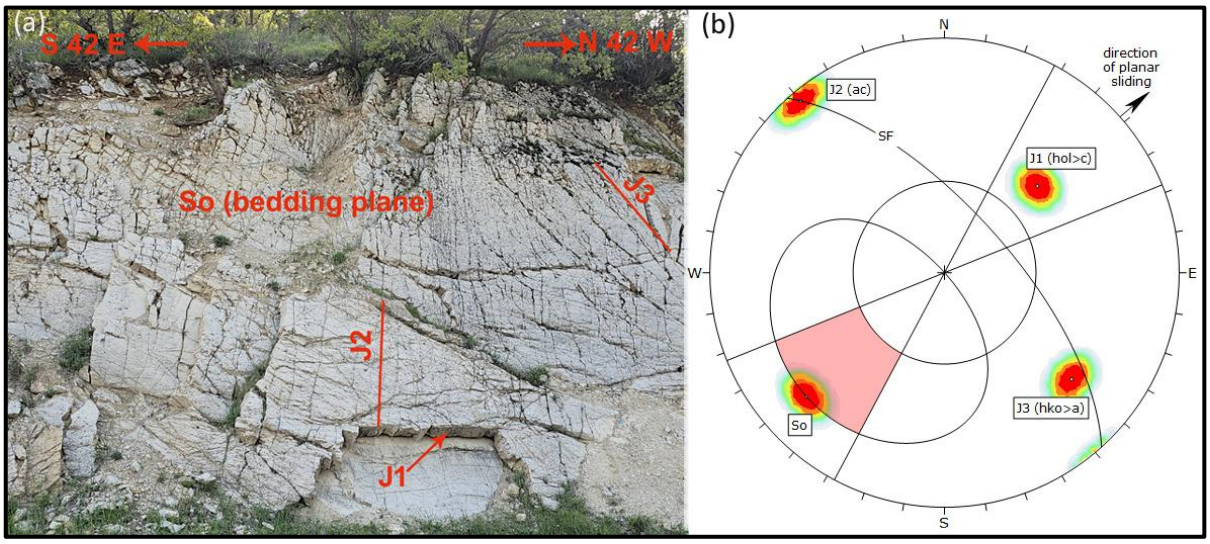

Figure 9. a) Photo of Station No. 4 with signs for discontinuity groups. b) Stereographic analysis displays planar sliding on So.

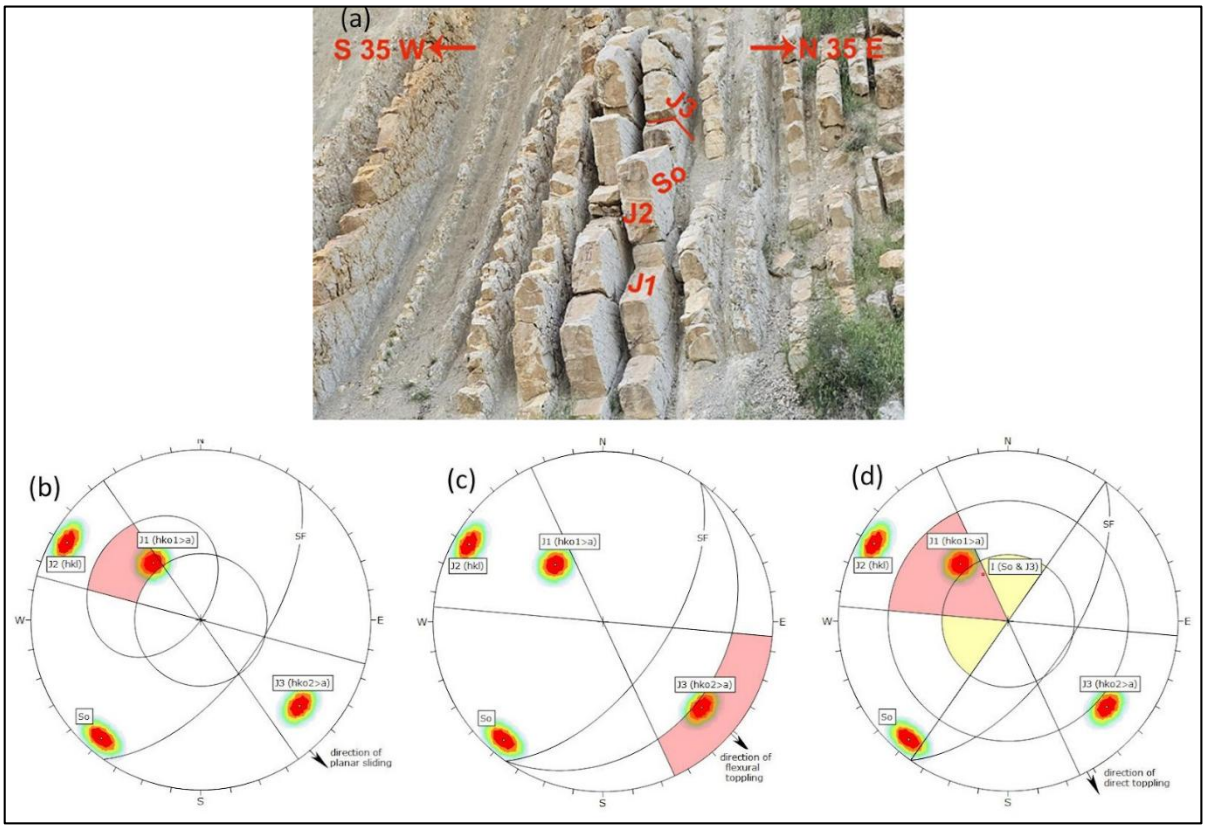

Figure 10. a) Photo of Station No. 5 with signs for discontinuity groups. b) Stereographic analysis displays planar sliding on J1. c) Flexural toppling about J3. d) Direct toppling through intersected planes (So & J3) with the aid of J1 as a basal plane.

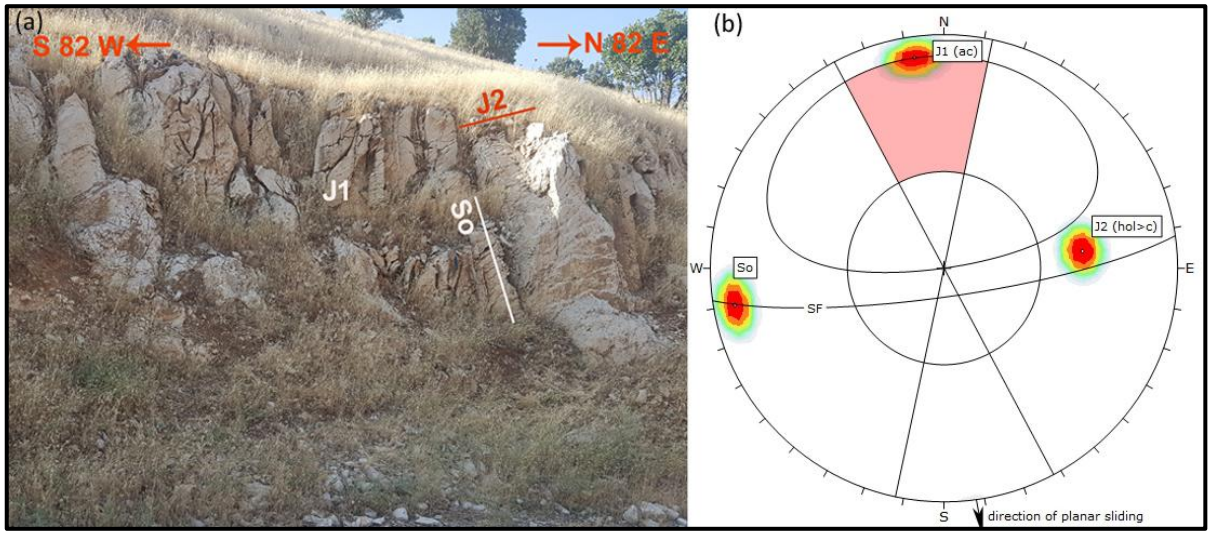

Figure 11. a) Photo of Station No. 6 with signs for discontinuity groups. b) Stereographic analysis displays planar sliding on J1.

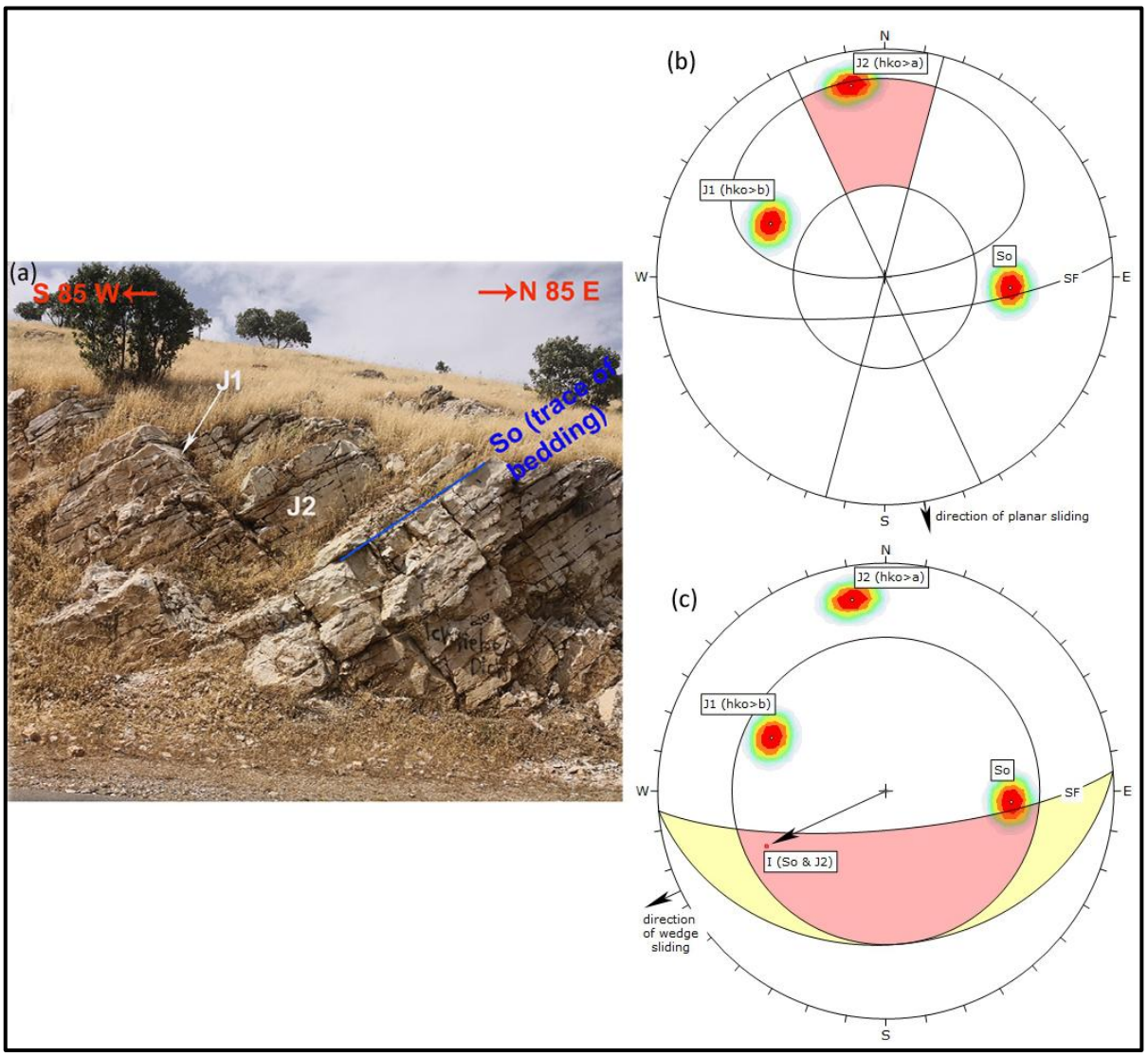

Figure 12. a) Photo of Station No. 7 with signs for discontinuity groups. b) Stereographic analysis displays planar sliding on J2. c) Wedge sliding on So and J2.

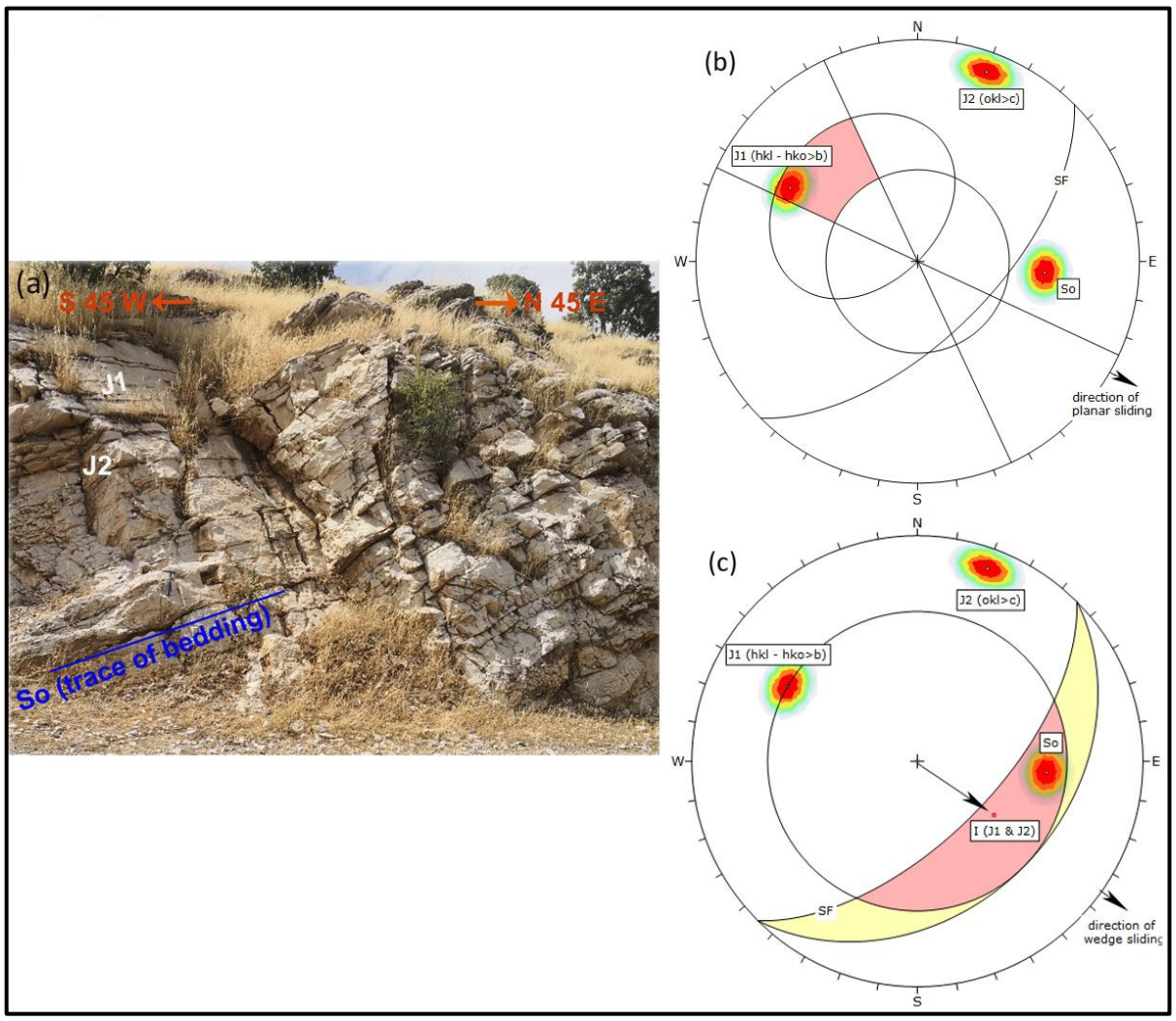

Figure 13. a) Photo of Station No. 8 with signs for discontinuity groups. b) Stereographic analysis displays planar sliding on J1. c) Wedge sliding on J1 and J2.

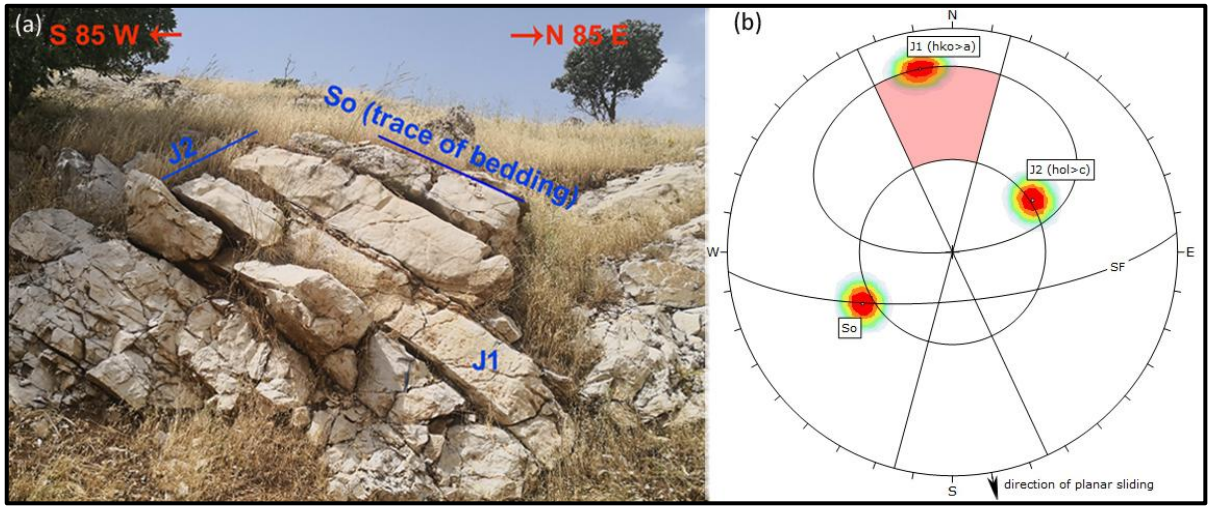

Figure 14. A-Photo of Station No. 9 with signs for discontinuity groups. B-Stereographic analysis displays planar sliding on J1.

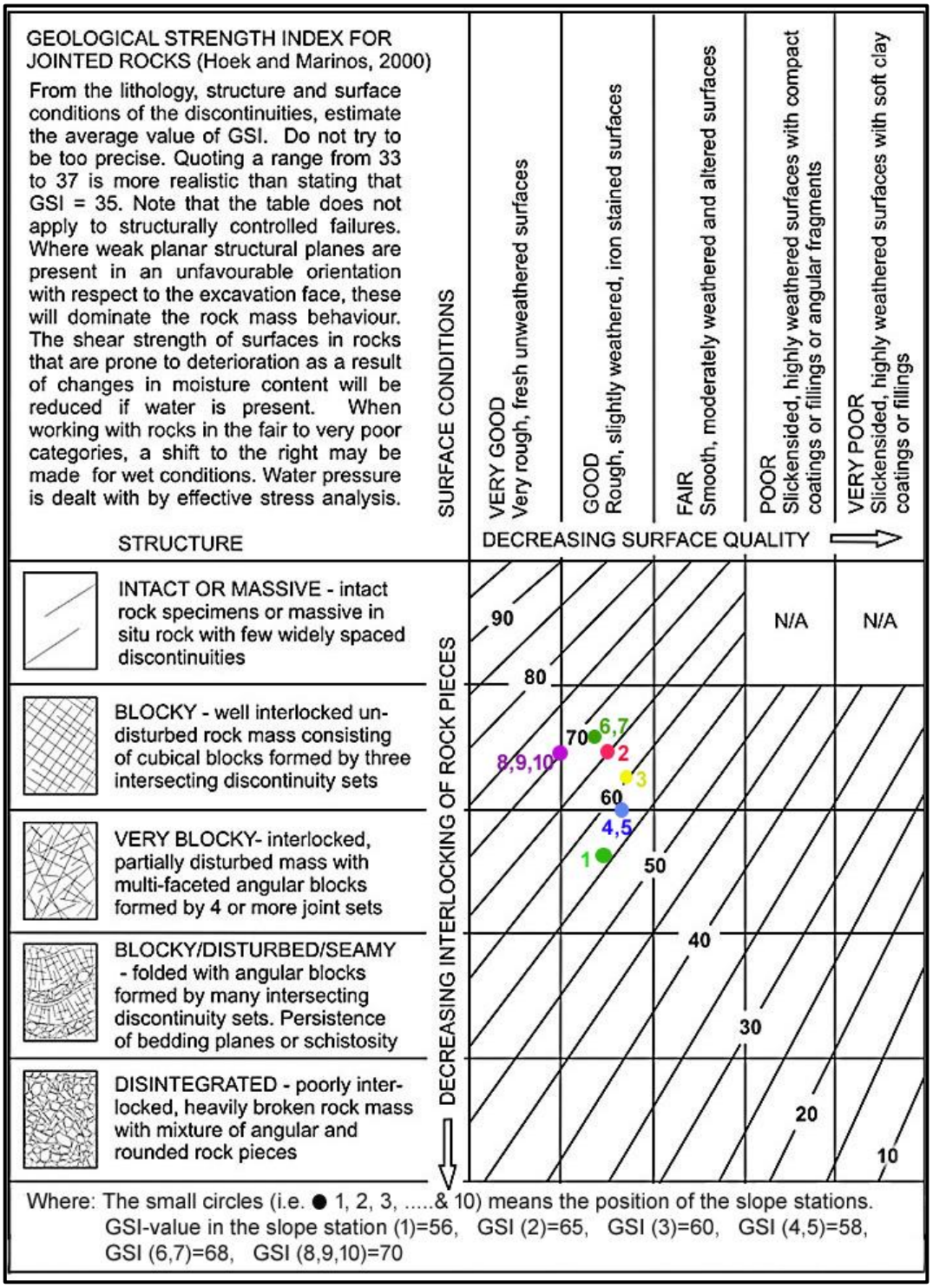

Figure 15. The rock mass's GSI values in the ten (10) slope stations (circles indicate the position of the rock mass in each station) (after Marinos and Hoek, 2000).

Table 4. Kinematic analysis results of rock slopes by DIPS-Software.

Slope station no.	Planar sliding & its direction	Wedge sliding & its direction	Flexural toppling & its direction	Direct toppling & its direction
1	Nil	√ (129°)	Nil	Nil
2	√ (087°)	Nil	Nil	Nil
3	√ (070°)	Nil	Nil	Nil
4	√ (048°)	Nil	Nil	Nil
5	√ (140°)	Nil	√ (131°)	√ (153°)
6	√ (160°)	Nil	Nil	Nil
7	√ (172°)	Nil	Nil	Nil
8	√ (170°)	√ (244°)	Nil	Nil
9	√ (120°)	√ (125°)	Nil	Nil
10	√ (170°)	Nil	Nil	Nil

GSI values can be estimated from field observation resulting from the combination of rock structure and joint conditions (roughness, weathering, and filling materials (AlJubory et al., 2022; Hasan & Abood, 2024; Hoek & Brown, 1997; V. Marinos et al., 2005; Narimani et al., 2023; Sadiq et al., 2016), and the results of the GSI values of the rock masses in the mentioned stations were estimated on Marinos and Hoek (2000) chart, as in Figure 16 and Table 5. The groundwater was considered in moist condition because most failures occurred in the winter and spring seasons, so the rating of seven (7) fits with this consideration according to Bieniawski (1976), not Bieniawski, (1973), as in Tables 5 and 6.

The GSI-slope of Hamasur (2023) was applied, utilizing GSI values of all the mentioned ten stations from Figure 16. The F1, F2, and F3 factors rating were calculated from Hamasur (2023) graphs Figures 5a, 5b, 5c, and 5d. Furthermore, these graphs require knowing the failure type, failure plane dip direction, and angle in the case of planar sliding and flexural toppling, plunge direction and angle in the case of wedge sliding and direct toppling, slope direction and its inclination angle, these elements were determined in the field and illustrated in Table 5.

After determining all the requirements, the GSI_{slope} values for all rock slope stations were calculated from the GSI_{slope} equation (Eq.1). The results of the GSI_{slope} displayed that stations no.3 and 5 are completely unstable slopes of class five (V), stations no. 1, 2, 4, 6, 7, 8, and 9 are unstable slopes of class four (IV), and station no 10 is partially stable of class three (III), as in Table 6.

Table 5. Required elements for determining the GSI-slope.

Station no.	GSI Value	Type of failure	Ground-water Condition	αs/ βs (Slope)	αj or αi	|αj – αs|, |αi – αs| or ||αj – αs| - 180|	βj or βi	βj – βs or βi – βs	βj + βs or βi + βs
1	**56**	**WS**	Moist in winter & spring	115°/60°	129°	14°	33°	- 27°	
2	**65**	**PS**	Moist in winter & spring	105°/60°	087°	18°	58°	- 2°	
3	**60**	**PS**	Moist in winter & spring	076°/53°	070°	6°	50°	- 3°	
4	**58**	**PS**	Moist in winter & spring	048°/68°	048°	0°	68°	0°	
		PS			140°	15°	36°	- 24°	
5	**58**	**FT**	Moist in winter & spring	125°/60°	311°	6°	66°		126°
		DT			333°	28°	65°		125°
6	**68**	**PS**	Moist in winter & spring	160°/80°	160°	0°	80°	0°	
7	**68**	**PS**	Moist in winter & spring	172°/80°	172°	0°	80°	0°	
		PS			170°	5°	74°	- 2°	
8	**70**		Moist in winter & spring	175°/76°					
		WS			244°	69°	42°	- 42°	
		PS			120°	15°	56°	- 6°	
9	**70**		Moist in winter & spring	135°/62°					
		WS			125°	10°	55°	- 7°	
10	**70**	**PS**	Moist in winter & spring	175°/72°	170°	5°	72°	0°	

Where PS = Planar sliding; WS = Wedge sliding; FT = Flexural toppling; DT = Direct toppling; αs = Slope dip direction; αj = Joint (discontinuity) dip direction; αi = Plunge direction of intersection line; βj = Joint (discontinuity) dip angle; βi = Plunge angle of intersection line; βs = Slope dip angle

Table 6. GSI values, Groundwater, F1, F2, F3 Rating, and GSI-slope results.

Station no.	GSI Value	Type of failure	WR	F1 Rating	F2 Rating	F3 Rating	F1.F2.F3	GSI-slope Value	GSI-slope Class / Stability
1	**56**	**WS**	7	0.72	0.74	-60	-32	21	lV / Unsta
2	**65**	**PS**	7	0.60	0.97	-43	-25	37	lV / Unsta
3	**60**	**PS**	7	0.88	0.95	-47	-39	18	V / CUnsta
4	**58**	**PS**	7	1	0.97	-30	-29	26	lV / Unsta
		PS		0.70	0.85	-60	-35.7	19.3	V / CUnsta
5	**58**	**FT**	7	0.88	1	-24	-21	34	lV / Unsta
		DT		0.36	1	-23.5	-8.5	46.5	III /Pasta
6	**68**	**PS**	7	1	0.99	-30	-29.7	35	lV / Unsta
7	**68**	**PS**	7	1	0.99	-30	-29.7	35	lV / Unsta
8	**70**	**PS**	7	0.90	0.98	-43	-37.9	29	lV / Unsta
		WS		0.01	0.88	-60	-0.5	66.5	II / Stab
9	**70**	**PS**	7	0.66	0.96	-57	-36	31	lV / Unsta
		WS		0.79	0.95	-59	-44	23	lV / Unsta
10	**70**	**PS**	7	0.90	0.97	-30	-26	41	III /Pasta

Where: PS = Planar sliding; WS = Wedge sliding; FT = Flexural toppling; DT = Direct toppling; F1, F2 & F3 are adjustment factors of GSI-slope; Pasta=Partially stable; Unsta = Unstable; CUnsta = Completely Unstable; WR = Groundwater Rating; GSI-slope = GSI – 10 + WR + (F1 x F2 x F3).

5. Conclusions

Kinematic analysis displayed that planar sliding is the most common mechanism of failure, the second type is wedge sliding, and toppling failures (flexural and direct toppling) are the least failure mechanisms that may occur. Minor (secondary) syncline in station no.1 controls the occurrence of wedge sliding on both limbs of the minor fold. The GSI_{slope} system is an easy and simple way to determine the degree of stability of the rock slopes, so rock slopes of stations no.3 and 5 are the most unstable (completely unstable) slopes, rock slopes of stations no.1, 2, 4, 6, 7, 8, and 9 are in dangerous of order two (unstable slopes), and station no.10 comes finally (partially stable slope).

References

Al-Bared, M. A. M., Harahap, I. S. H., Marto, A., Mustaffa, Z., Ali, M. O. A., & Al-Subal, S. (2019). Stability of cut slope and degradation of rock slope forming materials–a review. *Malaysian Construction Research Journal*, *6*(1), 215–228.

Al-Hakary, S. H. (2011). *H. Geometrical analysis and structural evolution of a selected area from NE Zagros Fold Thrust Belt and their tectonic implications, Northeast Iraq region, NE Iraq*. Sulaimani.

AlJubory, M. K., Abood, M. R., & Khider, M. E. (2022). Assessment of rock slope stability along Bazian-Basara main road, Sulaimani, NE Iraq. *The Iraqi Geological Journal*, 162–169.

Al-Jumaily, I. (2004). *Tectonic investigation of the brittle failure structures in the Foreland Folds Belt. Northern Iraq, Unpub*.

Al-Saadi, S. N. (1981). *A method for mapping unstable slopes with reference to the coast line of SW Dyfed, Wales.* University of Bristol.

Aziz, B., Lawa, F., & Said, B. (2001). Sulaimani seismic swarm during spring 1999, NE Iraq. *Journal of Zankoy Sulaimani-Part A*, *4*(1), 87–100.

Bar, N., & Barton, N. (2017). The Q-slope method for rock slope engineering. *Rock Mechanics and Rock Engineering*, *50*, 3307–3322.

Bienawski, Z. T. (1976). *Rock mass classifications in rock engineering.*

Bieniawski, Z. (1973). Engineering classification of jointed rock masses. *Civil Engineering Siviele Ingenieurswese*, *1973*(12), 335–343.

Bieniawski, Z. T. (1989). *Engineering rock mass classifications: A complete manual for engineers and geologists in mining, civil, and petroleum engineering*. John Wiley & Sons.

Bruce, I., Cruden, D., & Eaton, T. (1989). Use of a tilting table to determine the basic friction angle of hard rock samples. *Canadian Geotechnical Journal*, *26*(3), 474–479.

Buday, T. (1980). *The regional geology of Iraq: Stratigraphy and paleogeography* (Vol. 1). State Organization for Minerals, Directorate General for Geological Survey ….

Chakraborty, R., & Dey, A. (2019). *Effect of toe cutting on hillslope stability*. 191–198.

Fouad, S. F. (2015). Tectonic map of Iraq, scale 1: 1000 000, 2012. *Iraqi Bulletin of Geology and Mining*, *11*(1), 1–7.

Goodman, R. E. (1989). *Introduction to rock mechanics* (Vol. 2). Wiley New York.

Hamasur, G. A. (2013). Slope Stability Assessment within and around the Reservoir of the Proposed Basara Dam, Sulaimaniyah, NE Iraq. *Iraqi Bulletin of Geology and Mining*, *9*(3), 51–66.

Hamasur, G. A. (2022). Kinematic and Q-slope Application for Stability Assessment of the Rock Slopes Along Goshan_Qupy Qaradagh Road, Sulaimaniyah, NE-Iraq. *Jordan Journal of Earth & Environmental Sciences*, *13*(2).

Hamasur, G. A. (2023). Geological strength index-slope: An adaptation of the geological strength index system for use in the rock slope stability assessment. *Brazilian Journal of Geology*, *53*, e20220044.

Hamasur, G. A., Mohammed, F. O., & Ahmad, A. J. (2020). Assessment of Rock Slope Stability along Sulaimaniyah -Qaradagh Main Road, Near Dararash Village, Sulaimaniyah, NE-Iraq. *Iraqi Journal of Science*, 3266–3286. https://doi.org/10.24996/ijs.2020.61.12.15

Hamasur, G. A., & Qadir, N. M. (2020). Slope stability assessment along Qalachwalan-Suraqalat main road, Sulaimani, NE-Iraq. *Tikrit Journal of Pure Science*, *25*(3), 26–48.

Hancock, P. (1985). Brittle microtectonics: Principles and practice. *Journal of Structural Geology*, *7*(3–4), 437–457.

Hancock, P., Al Kadhi, A., & Sha'At, N. (1984). Regional joint sets in the Arabian platform as indicators of intraplate processes. *Tectonics*, *3*(1), 27–43.

Hancock, P., & Atiya, M. (1979). Tectonic significance of mesofracture systems associated with the Lebanese segment of the Dead Sea transform fault. *Journal of Structural Geology*, *1*(2), 143–153.

Hasan, A. I., & Abood, M. R. (2024). Rock Slopes Stability Analysis along the Qaywan-Mokba Road in Sulaymaniyah Governorate, Northeastern Iraq. *The Iraqi Geological Journal*, 91–106.

Hocking, G. (1976). A method for distinguishing between single and double plane sliding of tetrahedral wedges. *International Journal of Rock Mechanics and Mining Science*, *13*(Analytic).

Hoek, E., & Bray, J. D. (1981). *Rock slope engineering*. CRC Press.

Hoek, E., & Brown, E. T. (1997). Practical estimates of rock mass strength. *International Journal of Rock Mechanics and Mining Sciences*, *34*(8), 1165–1186.

Hostani, B. A., & Hamasur, G. A. (2022). Kinematic and Slope Mass Rating Application for Rock Slope Stability Evaluation Along Shanadar-Goratu Road in the Gali-Ashkafte Valley, Erbil, NE-Iraq. *The Iraqi Geological Journal*, 59–81.

Huang, F., Yan, J., Fan, X., Yao, C., Huang, J., Chen, W., & Hong, H. (2022). Uncertainty pattern in landslide susceptibility prediction modelling: Effects of different landslide boundaries and spatial shape expressions. *Geoscience Frontiers*, *13*(2), 101317. https://doi.org/10.1016/j.gsf.2021.101317

Hussien, S. A., Al-Kubaisi, M. S., & Hamasur, G. A. (2020). Impact of Geological Structures on Rock Slope Stability in The NW Nose (Plunge) of Surdash Anticline, Sulaimaniya/NE Iraq. *Iraqi Journal of Science*, 550–566.

Janardhana, M., Abdul-Aleam, A., & Al-Qadhi, A. (2018). Slope stability assessment in and around Taiz city, Yemen using Landslide Possibility Index (LPI). *Eur J Adv Eng Technol*, *5*(1), 8–17.

Jassim, S. Z., & Goff, J. C. (2006). *Geology of Iraq*. DOLIN, sro, distributed by Geological Society of London.

Karim, K. H., & Ahmad, S. H. (2014). Structural analysis of the Azmir–Goizha anticline, north and northeast of Sulaimani city, Kurdistan Region, Northeast Iraq. *Journal of Zankoy Sulaimani-Part A (JZS-A)*, *16*(1), 1.

Lawa, F. A., Koyi, H., & Ibrahim, A. (2013). TECTONO-STRATIGRAPHIC EVOLUTION OF THE NW SEGMENT OF THE ZAGROS FOLD-THRUST BELT, KURDISTAN, NE IRAQ. *Journal of Petroleum Geology*, *36*(1), 75–96. https://doi.org/10.1111/jpg.12543

Malviya, D. K., Samanta, M., Dash, R. K., & Kanungo, D. P. (2024). Anthropogenically induced instability in road cut slopes along NH-39, Manipur, North-East Indian Himalaya: Assessment and mitigation measures. *Environment, Development and Sustainability*, *26*(3), 6239–6268.

Marinos, P., & Hoek, E. (2000). GSI: a geologically friendly tool for rock mass strength estimation. *ISRM International Symposium*.

Marinos, V., & Carter, T. G. (2018). Maintaining geological reality in application of GSI for design of engineering structures in rock. *Engineering Geology*, *239*, 282–297.

Marinos, V., Marinos, P., & Hoek, E. (2005). The geological strength index: Applications and limitations. *Bulletin of Engineering Geology and the Environment*, *64*(1), 55–65.

Markland, J. T. (1972). *A useful technique for estimating the stability of rock slopes when the rigid wedge slide type of failure is expected*. Interdepartmental Rock Mechanics Project, Imperial College of Science and ….

Meena, M. K., Singh, A. K., Dwivedi, R. D., & Mohnot, J. K. (2025). Failure Mechanism of a Large Wedge in Open Cast Mine Composed of a Granite Porphyry Rock Mass of Aravali Region-A Case Study. *Journal of Rock Mechanics and Tunnelling Technology (JRMTT)*, *31*(1), 31–43.

Mohammed, F. O., Ahmed, A. J., & Mohammed, S. H. (2020). Landslide susceptibility assessment along Biyara-Tawella road, Kurdistan region, NE-Iraq. *Zankoy*, *22*(1), 1–38.

Mohammed, F. O., Hamasur, G. A., & Almanmi, D. A. (2023). Rock Mass Strength Analysis and Disturbance Factor Estimation of Heterogeneous Rock Masses for the Dam Foundation: A Case Study at Kanarwe River Basin, Kurdistan Region, NE-Iraq. In R. E. Hammah, S. Javankhoshdel, T. Yacoub, A. Azami, & A. McQuillan (Eds.), *Proceedings of the Rocscience International Conference 2023 (RIC2023)* (Vol. 19, pp. 233–244). Atlantis Press International BV. https://doi.org/10.2991/978-94-6463-258-3_25

Narimani, S., Davarpanah, S. M., Bar, N., Török, Á., & Vásárhelyi, B. (2023). Geological strength index relationships with the Q-system and Q-slope. *Sustainability*, *15*(14), 11233.

Numan, N. M. (1997). A plate tectonic scenario for the Phanerozoic succession in Iraq. *Iraqi Geological Journal*, *30*(2), 85–110.

Omar, A. A., Lawa, F. A., & Sulaiman, S. H. (2015). Tectonostratigraphic and structural imprints from balanced sections across the north-western Zagros fold-thrust belt, Kurdistan region, NE Iraq. *Arabian Journal of Geosciences*, *8*(10), 8107–8129. https://doi.org/10.1007/s12517-014-1682-6

Pantelidis, L. (2009). Rock slope stability assessment through rock mass classification systems. *International Journal of Rock Mechanics and Mining Sciences*, *46*(2), 315–325.

Priest, S. D. (1993). *Discontinuity analysis for rock engineering*. Springer Science & Business Media.

Qader, R. M., & Syan, S. H. A. (2021). Rock slope stability assessment along Rawanduz main road, Kurdistan Region. *The Iraqi Geological Journal*, 79–93.

Ramsay, J. G., & Huber, M. I. (1987). Modern structural geology. *Folds and Fractures*, *2*, 309–700.

Rocscience (Version 6). (2015). [Computer software].

Romana, M. (1985). New adjustment ratings for application of Bieniawski classification to slopes. *Proceedings of the International Symposium on Role of Rock Mechanics, Zacatecas, Mexico*, 49–53.

Sadiq, S., Muhmed, A. S., Haris, H. G. K., Hamma, D. M., Abdwllah, M. M., Bibani, H. H., Muhealddin, H. K., Mustafa, H. A., Sissakian, V., & Al-Ansari, N. (2016). Mechanism of Haibat Sultan Mountain landslide in Koya, North Iraq. *Engineering*, *8*(8), 535–544.

Sharma, M., Sharma, S., Kumar, M., & Singh, S. (2019). Analysis of slope stability of road cut slopes of Srinagar, Uttrakhand, India. *Int J Appl Eng Res*, *14*(3), 609–615.

Singh, B., & Goel, R. K. (1999). *Rock mass classification: A practical approach in civil engineering* (Vol. 46). Elsevier.

Stevanovitic, Z., Miroslav, M., & Markovitic, Y. (2003). Hydrogeology of Northern Iraq, UN. *FAO Report*, *1*, 225p.

Turner, F. J., & Weiss, L. E. (1963). Structural analysis of metamorphic tectonics.

About the authors

Prof. Dr. Ghafor Ameen Hamasur earned his B.Sc. in Geology from Salahaddin University in 1987, followed by an M.Sc. in Engineering Geology from the same university in 1991. He later completed his Ph.D. in Geology (Engineering Geology) at the University of Sulaimani in 2009, focusing on rock slope stability and rock mass engineering.He began his academic career at the University of Sulaimani, where he currently serves as a professor of engineering geology in the Department of Earth Sciences, College of Science. His research interests include engineering geological evaluation of dam site foundations, tunnels, and rock slopes, as well as fracture analysis within the field of structural geology.

e-mail: ghafor.hamasur@univsul.edu.iq

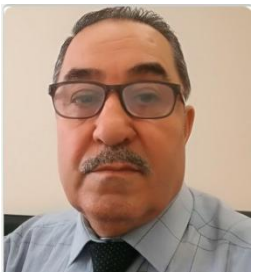

Prof. Dr. Salim Hasan Suleiman Al-Hakari earned a bachelor's degree in 1989 and a master's degree in 1993, both from the University of Mosul, specializing in structural geology with a focus on paleo stress analysis. He began his academic career as a lecturer assistant at the University of Sulaimani in 2004. In 2011, he completed his Ph.D. at the same university, researching the geometry of folds around Sulaymaniyah City. Currently, he holds the position of professor in structural geology. His research contributions include eleven published papers on paleo stress analysis and fold geometry.

Assit Prof. Dr. Fahmy Osman Mohammed began his academic journey at the University of Sulaimani, earning a Bachelor of Science in Geology in 2005. He continued his studies there, specializing in Engineering Geology with a Master's degree in 2011. Most recently, in 2023, he completed his Ph.D. within the Geology Department at the same university. Dr. Mohammed brings 15 years of experience to the fields of Engineering Geology, Environmental Modeling, Remote Sensing, and GIS. His expertise is further demonstrated by his ten published articles on various geological topics.